The role of aerosols and meteorological conditions in shaping cloud droplet development in New Mexico summer deep-convective systems

Huihui Wu[1*], Nicholas Marsden[2], Paul Connolly[1], Michael Flynn[1], Paul I. Williams[2], Declan Finney[3], Kezhen Hu[1], Graeme J. Nott[4], Navaneeth Thamban[1], Keith Bower[1], Alan Blyth[3], Martin Gallagher[1] and Hugh Coe[1,2]

[1]Department of Earth and Environmental Sciences, University of Manchester, Manchester, UK
[2]National Centre for Atmospheric Science, University of Manchester, Manchester, UK
[3]School of Earth & Environment, University of Leeds, Leeds, UK
[4]FAAM Airborne Laboratory, Cranfield, UK
*Now at: Univ Paris Est Créteil and Université Paris Cité, CNRS, LISA, 94010 Créteil, France

Correspondence to: Hugh Coe (hugh.coe@manchester.ac.uk)

Supplement

Table S1. Summary of the data availability for aerosol and cloud instruments.

Flight ID	Date	AMS	SP2	SMPS	PCASP	CPC	CDP
C297	16/07/2022	N	Y	N	Y	Y	Y
C298	19/07/2022	N	Y	Y	Y	Y	Y
C299	20/07/2022	Y	Y	Y	Y	Y	Y
C300	22/07/2022	Y	Y	Y	Y	Y	Y
C301	23/07/2022	Y	Y	N	Y	Y	Y
C302	24/07/2022	Y	Y	Y	Y	Y	Y
C303	25/07/2022	Y	Y	Y	Y	Y	Y
C304	26/07/2022	(Y)	Y	Y	Y	Y	Y
C305	27/07/2022	Y	Y	Y	Y	Y	Y
C306	29/07/2022	Y	Y	Y	Y	Y	Y
C307	30/07/2022	Y	Y	Y	Y	Y	Y
C308	31/07/2022	Y	N	Y	Y	Y	Y
C309	01/08/2022	Y	Y	Y	Y	Y	Y
C310	02/08/2022	Y	Y	Y	Y	Y	Y
C311	03/08/2022	N	Y	Y	Y	Y	Y
C312	04/08/2022	N	Y	Y	Y	Y	Y
C313	06/08/2022	Y	Y	(Y)	Y	Y	Y
C314	07/08/2022	(Y)	(Y)	Y	Y	Y	Y
C315	08/08/2022	N	N	Y	Y	Y	Y

Note: N represent unavailable data, Y represent available data, (Y) represent not completely available data.

Table S2. Summary of cloud properties in the lowest measured clouds and below-cloud aerosols.

Flight ID	Date	below-cloud N_a, cm^{-3}	N_d, cm^{-3}	LWC, $g\ m^{-3}$	R_e, μm	Approximate Distance (m)
C298	19/07/2022	632±172 (highest: 1439)	722±230 (highest: 1045)	0.10±0.04	3.2±0.2	−30
C299	20/07/2022	533±129 (1472)	609±345 (1055)	0.09±0.06	3.3±0.1	−150
C300	22/07/2022	636±200 (1490)	543±342 (1015)	0.12±0.08	3.8±0.1	−90
C301	23/07/2022	556±157 (1198)	521±290 (777)	0.13±0.07	4.1±0.0	120
C303	25/07/2022	770±86 (1070)	487±163 (663)	0.78±0.42	8.1±0.4	500
C304	26/07/2022	412±49 (508)	345±197 (593)	0.45±0.38	7.8±0.6	540
C305	27/07/2022	619±188 (1202)	886±317 (1292)	0.27±0.10	4.3±0.2	−200
C306	29/07/2022	707±134 (1081)	498±284 (1030)	0.61±0.39	7.4±0.7	400
C307	30/07/2022	526±59 (665)	500±233 (860)	0.79±0.44	7.9±0.3	600
C308	31/07/2022	298±109 (531)	320±134 (860)	0.41±0.26	7.3±0.9	500
C309	01/08/2022	555±95 (892)	680±314 (1285)	0.35±0.23	5.1±0.6	280
C310	02/08/2022	521±155 (1216)	669±375 (974)	0.15±0.09	3.8±0.1	−40
C312	04/08/2022	859±235 (1239)	591±248 (1018)	0.50±0.32	6.2±0.7	120
C313	06/08/2022	642±177 (962)	524±244 (969)	0.16±0.09	4.3±0.7	10
C314	07/08/2022	795±166 (1097)	823±296 (1025)	0.19±0.07	3.9±0.1	−230

Note: The distances are approximate distances between the lowest measured cloud layers and the LCL heights.

Table S3. Experimental conditions used for case studies.

Exp.	Initial T (K)	Initial P (hpa)	RH (%)	kappa	Size mode	Initial updraft velocity (m/s)	Initial parcel radius
Period 1-C300 case	277	576.45	52	0.27	Mode1	2.5	500
Period 2-C303 case	282	650.17	67	0.41	Mode2	2.5	500

Note: The setup of initial T, P and RH, and aerosol characteristics (kappa and size modes) are selected from two flights (C300 and C303). Aerosol size distributions were averaged over near cloud-base SLRs. The size modes are displayed in Fig. S7. The initial T, P and RH were averaged within 200 m below the LCL height.

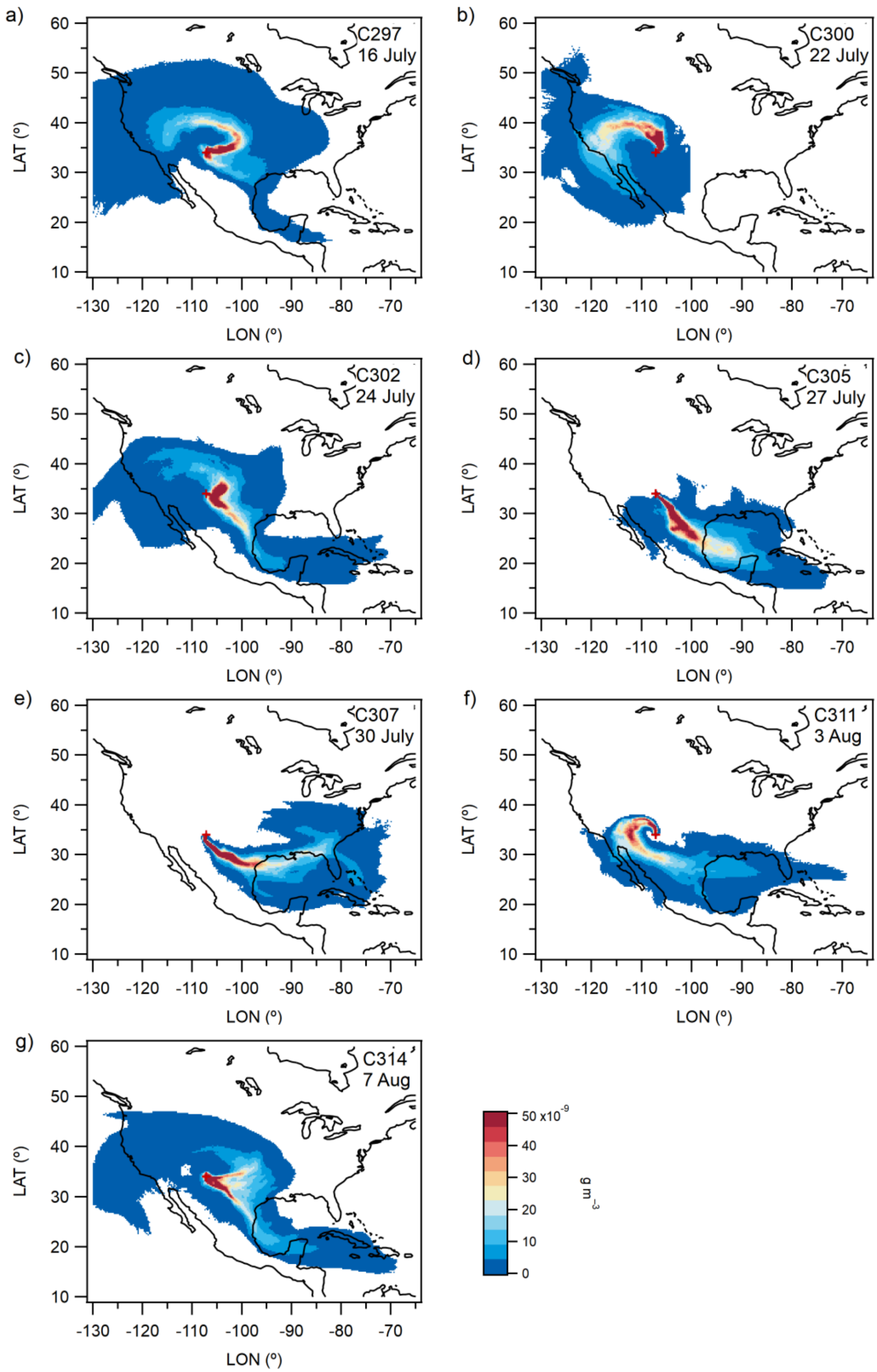
a)
C297
16 July
b)
C300
22 July
c)
C302
24 July
d)
C305
27 July
e)
C307
30 July
f)
C311
3 Aug
g)
C314
7 Aug
LAT (°)
LON (°)
60
50
40
30
20
10
-130
-120
-110
-100
-90
-80
-70
50 x10⁻⁹
40
30
20
10
0
g m⁻³

Figure S1: Examples of backward-dispersion fields from selected flight simulations, illustrating different and representative horizontal footprints of original air parcels transported over the past six days before reaching the sampling area during the campaign. The corresponding flight numbers and dates are indicated in the upper right corner of each plot. The release area is marked with a red cross.

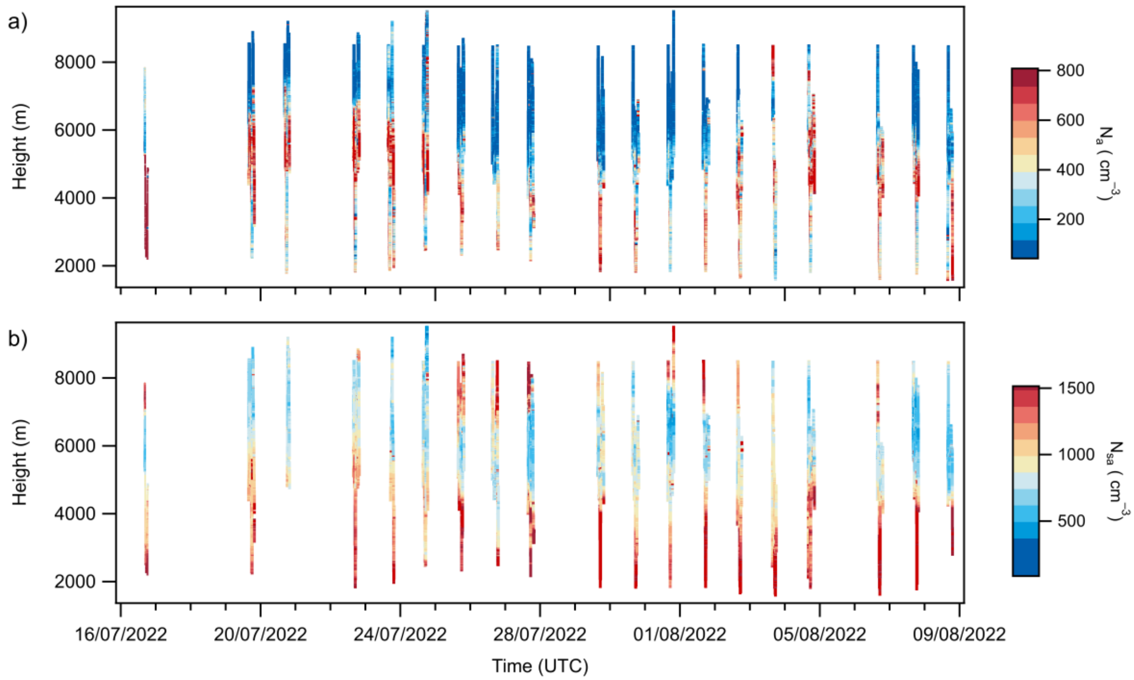

Figure S2. Vertical profiles of a) out-of-cloud N_a (0.1 to 3 µm) number concentrations from PCASP measurements and b) out-of-cloud CN_3 (3 nm to 1 µm) number concentrations from CPC measurements, for each flight.

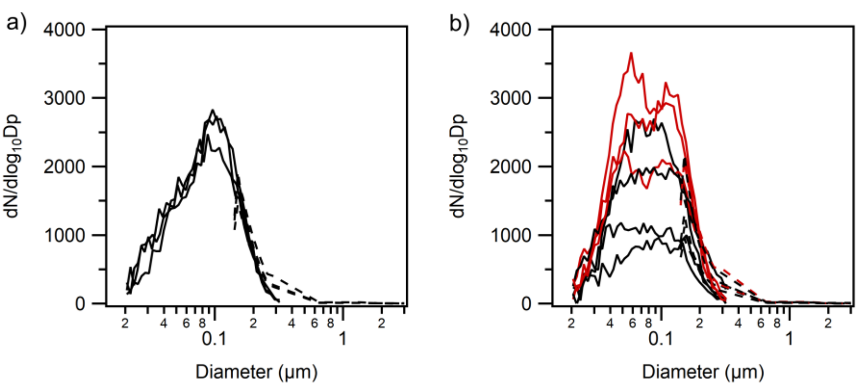

Figure S3. Average size distributions over near cloud-base SLRs for each single flight in Period 1 a) and Period 2 b). The solid lines represent results from SMPS, and the dashed lines represent results from PCASP. The red lines in b) highlight the bimodal size distributions with a distinct minimum between the two modes.

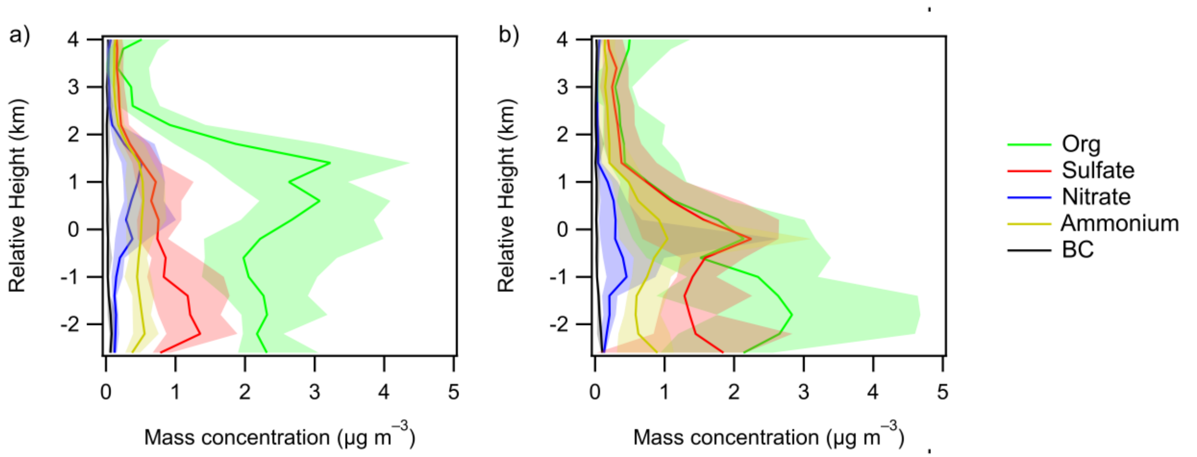

Figure S4. Average vertical profiles of mass concentrations of different chemical components out-of-cloud in a) Period 1 and b) Period 2. The lines and shades represent average and one standard deviation. The y-axis is the relative height with respect to the LCL height.

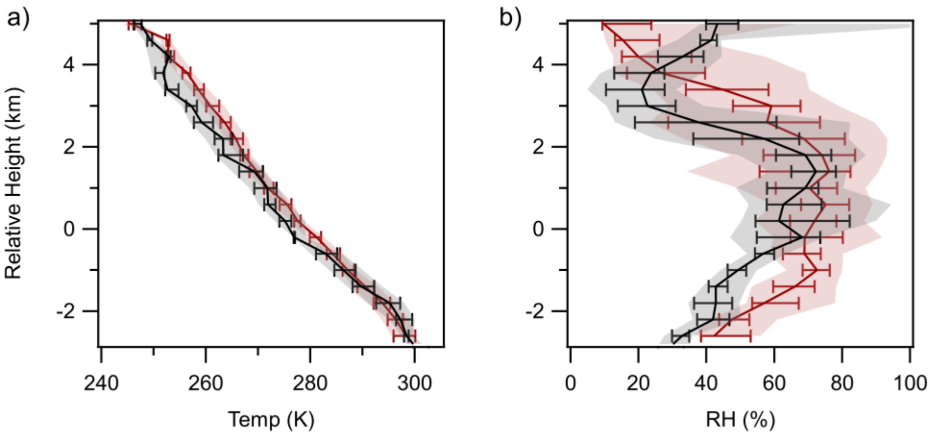

Figure S5. Vertical profiles of a) temperature (K) and b) RH (%). Black values represent results from Period 1, and red values represent results from Period 2. The lines, bars and shades represent median, 10, 25, 75, and 90 percentiles. The y-axis is the relative height with respect to the LCL height.

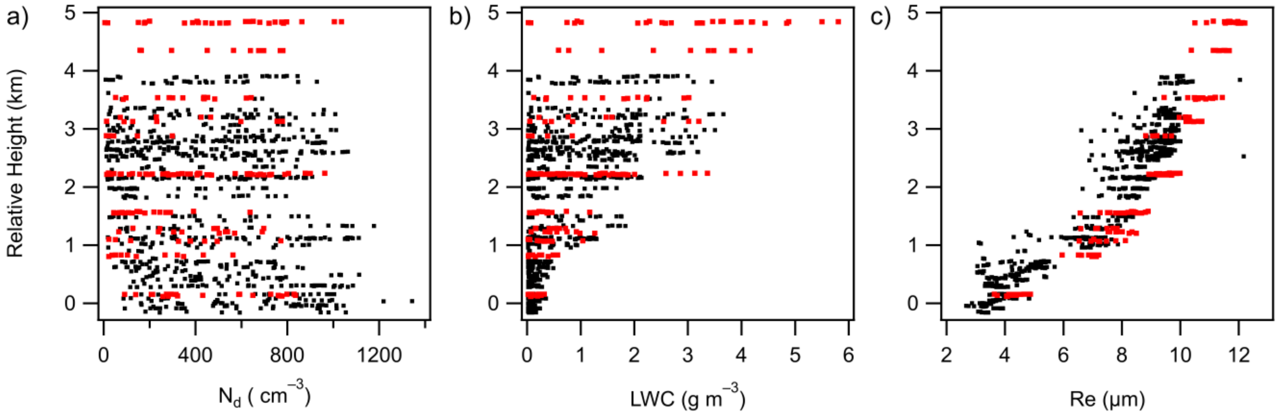

Figure S6. Vertical profiles of a) cloud droplet number concentration (N_d, cm^{-3}), b) liquid water content (LWC, g m^{-3}), and c) effective radius (R_e, μm) for Period 1 earlier flights (black, C298-C300) and C301 (red). The dots represent 1-hz measurements. The y-axis is the relative height with respect to the LCL height.

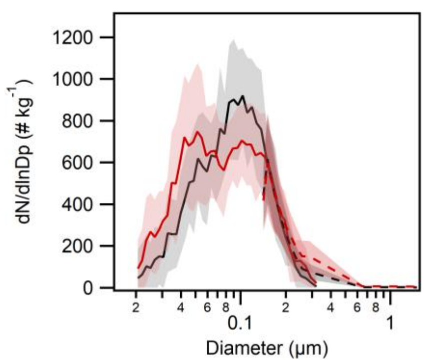

Figure S7: Aerosol size distribution (lines: averages; shades: standard deviations) for the Period 1-C300 case (Mode 1, black) and the Period 2-C303 case (Mode 2, red) for bin-microphysical parcel model simulations. The solid lines represent average results from SMPS, and the dashed lines represent average results from PCASP.